The interpretation of granitic textures from serial thin sectioning, image analysis and three-dimensional reconstruction

D. N. Bryon, M. P. Atherton and R. H. Hunter

Department of Earth Sciences, University of Liverpool, Brownlow Street, Liverpool, L69 3BX, UK

Abstract

Textural development of the felsic phases in two granodioritic rocks from the zoned Linga superunit of the Peruvian Coastal Batholith has been characterized using serial thin sectioning, image analysis and three-dimensional reconstruction. The study has shown how each mineral phase contributed to the texture during the formation and development of a contiguous crystal framework and during subsequent restriction, isolation and occlusion of the melt-filled porosity. The work highlights the important factors and potential problems in the use of serial thin sections and imaging in the analysis of complex polyphase rock textures.

Keywords: texture, granite, image analysis, serial thin section, Peru.

Introduction

An understanding of igneous rock textures is fundamental to the interpretation of magma chamber fluid dynamic and chemical processes, and thermal history. Generally, microscopic studies of the textures of igneous rocks involve examination in thin section, and much of the important granulometric information (e.g. grain size, shape, orientation, etc.) can be extracted by standard stereological analysis using orthogonal two-dimensional (2-D) sections. The interpretation of more complex information on the development of the texture during solidification requires an understanding of the texture in three-dimensions (3-D). To date such work has involved the careful study and interpolation of 2-D sections cut through the texture in various orientations. The main problem with this technique is that individual crystals in the sections do not relate to each other, and hence nothing is known of the detailed 3-D relationship between neighbouring crystals through the texture. Such information is critical to understanding the localized occlusion of the melt volume during cooling and crystallization, and hence such problems as melt extraction and magma evolution. In this contribution we concentrate on interpreting the geometry of specific phases through the texture from serial thin sections.

Serial thin sectioning and/or grinding and imaging have not been utilized as general methods in the analysis of igneous rock textures in the past. Such an approach is used in this contribution to interpret the textural evolution of two granitic rocks in 3-D. We describe briefly the sample preparation, imaging, processing and data-presentation techniques, and highlight the problems of extracting 3-D textural information from 2-D slices. Aspects of the crystallization history of the two rocks are discussed, and related to crystallization pathways in the quaternary An–Ab–Or–Qz system.

The samples on which this contribution is based are from two different traverses (the Arequipa and Yauca traverse) across the Linga Superunit of the Coastal Batholith of Peru. The samples were selected because they show textures which are typical of Cordilleran I-type granitic rocks (Atherton, 1981). In addition, the high level of emplacement of the Batholith (Atherton and Brenchley, 1972), and absence of deformation and secondary alteration have resulted in the preservation of the primary magmatic textures. Both rocks lie in the granodiorite field in the QAP Streckeisen diagram (Streckeisen,

Mineralogical Magazine, June 1995, Vol. 59, pp. 203–211

1976), but do show significant subtle differences in the abundance of several of the major phases. These differences are also seen in the textures, which vary in both two- and three-dimensions. The detailed petrography and chemistry of the samples are given by Atherton and Sanderson (1985) and Bryon *et al.* (1994), and are similar to those found in many of the superunits of the Peruvian Coastal Batholith (Atherton *et al.*, 1979). Briefly, the crystallization history involves early growth of plagioclase and amphibole with subsequent biotite, quartz and alkali feldspar saturation. The present study focuses on the felsic mineralogy, specifically, the development of a crystal framework of plagioclase feldspar and the subsequent timing of nucleation and growth of quartz and alkali feldspar, and on geometrical aspects of the reduction of the melt-filled porosity during crystallization.

Definition of textural elements and scale

At the outset of any analysis of texture or microstructure, it is necessary to establish what textural elements are important in order to understand any particular problem. In studies of geological (and non-geological) materials, grain boundaries and growth zones are important textural elements (e.g. Hunter, 1987; Means and Park, 1994). Boundaries define the shapes of grains and allow distinction to be made between early and late-stage growth on the rims of crystals. Growth zones within crystals, or boundaries between crystals and syntaxial overgrowths relate to stages in the cooling and cementation history of a rock.

The identification and filtering of textural elements using sophisticated automated image analysers is a general problem. Potentially, the advent of rapid high-resolution image collection and processing hardware, and a diverse array of analysis software can facilitate this. However, as with many forms of image, transmitted light images of all but the simplest rocks contain too much information to allow accurate definition of textural elements, such as grain boundaries, without significant filtering. With training, the human eye and brain does this rapidly and expertly. The problem is to program a computer to recognize what is important in the texture and discard unimportant information, i.e., 'noise'. This is a particular problem in igneous rocks such as granites, which contain several mineral phases that may have similar optical properties. This is compounded in many textures by the presence of secondary features such as cracks, lattice disorders, and post-solidification deformation and alteration which can only be distinguished by the trained eye. In our experience, as much time is spent manually filtering and cleaning automatically-digitized images as in identifying and manually digitising relevant and useful information directly from the section. In this study we have adopted the latter approach.

After defining the parameters of interest, in this case the grain boundaries, it is necessary to define the scale of observation required to understand a particular problem. This study was directed at understanding the 3-D spatial relationships and reconstruction of mm-sized textural elements on a scale of cm. This is reliant on the ability to trace individual crystals and textural elements through consecutive sections (using features such as optical continuity, similar geometries, extinction angles, zoning patterns, twin planes, etc.). The technique has no advantage over standard thin section studies if crystals appear in only one of the serial sections. Consequently, it was necessary to define the incremental spacing interval in the z direction. It is important to note that the lower limit defined by the constraints of the annular saw used in this study is 300 μm. Spatial interpolation of textural elements smaller than the 300 μm spacing cannot be reconstructed with any degree of confidence using serial thin sections generated in the method described here. Such features can, however, be examined using serial lapping/polishing (see Cooper and Hunter, this volume). Sectioning intervals of 300–500 μm proved ideal for the grain-size of our samples because it generated over 10 consective slices through the larger crystals (5–10 mm), as well as allowing crystals under 2 mm to be traced through several sections.

Sample preparation and image acquisition

Serial thin sections of the granodiorite samples were generated from 2 cm cubes of rock using a modified Malvern Instruments annular saw. Mutually perpendicular surfaces were cut prior to serial sectioning in order to facilitate re-alignment and orientation of successive slices during imaging. Sections were cut at intervals of 500 μm and subsequently lapped to a thickness of 40 μm. To enhance the distinction between alkali and plagioclase feldspar during digitization, all sections were stained with sodium cobaltinitrite. Images of each section were captured in plane-polarized transmitted light using a CCTV camera mounted on a Wild photomacroscope. They were digitized as 16 grey-level, 256 × 256 pixel, black and white images and stored as ASCII files on an OPUS-V PC. Optical alignment of successive thin sections prior to imaging was achieved with a precision of ~ 10 μm using corners and perpendicular edges; further adjustments could be made using software after image acquisition. For each slice, grain boundaries were traced and digitized manually using an optical mouse, and recorded as 2-D co-ordinate files of polygon networks.

Identification of individual grains through consecutive slices required simultaneous viewing of the original thin section in both PPL and XPL. The 2-D polygon networks were stacked into 3-D matrices and viewed as stereo pairs on a colour PGA; the pairs were generated by rotation of each stack by 4° about the vertical in the x-plane. Individual polygons in each section were colour-coded and information about individual grains extracted and viewed independently of other grains by switching colours to background. Images were either plotted as stacked stereo pairs (see Cooper and Hunter, this volume), or converted to Hewlett Packard Graphics (HPG) files and represented as consecutive two dimensional images within an Apple Macintosh graphics package (e.g. Canvas). All the images in this contribution are in the latter format, although 3-D stacked views of specific textural elements are presented in Figs. 4 and 6.

Textural development

The classic terminology developed by Wager *et al.* (1960) to describe cumulates in basic igneous rocks was a milestone in textural studies, and continues to form the backbone of our current understanding of the relationship between textural development and melt movement in basic igneous systems (e.g. Hunter, 1987). However, it is only recently that a coherent model to describe textural development in Cordilleran granitic rocks has been established (Bryon *et al.*, 1994). Three critical stages in the relationship between crystals and melt during static crystallization of a granitic magma can be identified (summarized in Fig. 1). Stage 1 involves the nucleation and growth of crystals in suspension in the magma. Continued growth leads to localized impingement between neighbouring crystals (Stage 1.2/3), which eventually results in the development of a contiguous framework of crystals (Stage 2). All subsequent crystallization from the melt occurs in the interstices of the framework (Stage 3), and may take the form of overgrowths on the margins of framework crystals and/or nucleation and growth of new crystals in the interstitial pore spaces. Of particular importance in the late stage evolution of the texture is the restricted inter-connectivity of the porosity and the local isolation of pore volumes (Stage 3.3). Within any specific silicic magma lineage, it is important to identify the role of individual mineral phases in each of these stages. This, in conjunction with detailed analysis of mineral chemical variations, provides a framework for interpreting melt evolution and the possible relative movement of melt and/or solid during crystallization (e.g., as a result of compositional convection and/or compaction). Aspects of the crystallization history of the two Peruvian granodiorites are discussed in relation to the general model outlined above, using the results obtained from the serial thin sectioning and image reconstructions.

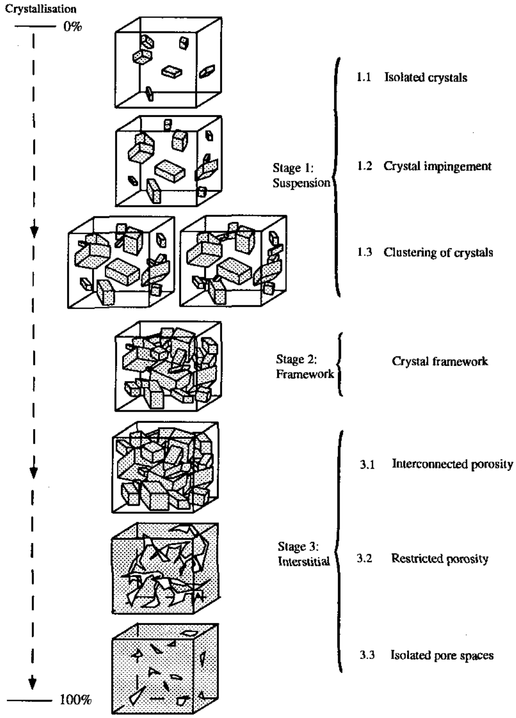

FIG. 1. (modified from Fig 4. in Bryon *et al.*, 1994). Breakdown of the crystallization into three stages based on the changing geometrical relationships that might be expected between crystals and melt during solidification. Crystals that initially grow in isolation from one another will start to impinge and interconnect as the volume of solid material increases (Stage 1). Eventually the crystals will form a continuous interconnecting framework (Stage 2). All subsequent crystallization will occur in the pore spaces in the interstices of the framework (Stage 3). Initially the interstitial melt is likely to remain connected, however, continued crystallization will reduce the pore volume and lead to the local isolation of individual pore spaces.

Textural relations in two dimensions

Photomicrographs of textures of the two granodiorites in thin section are shown in Plate 3 (see colour plate section). Although differing in detail, the morphology of the plagioclase and quartz crystals in each of the samples is similar. Plagioclase forms

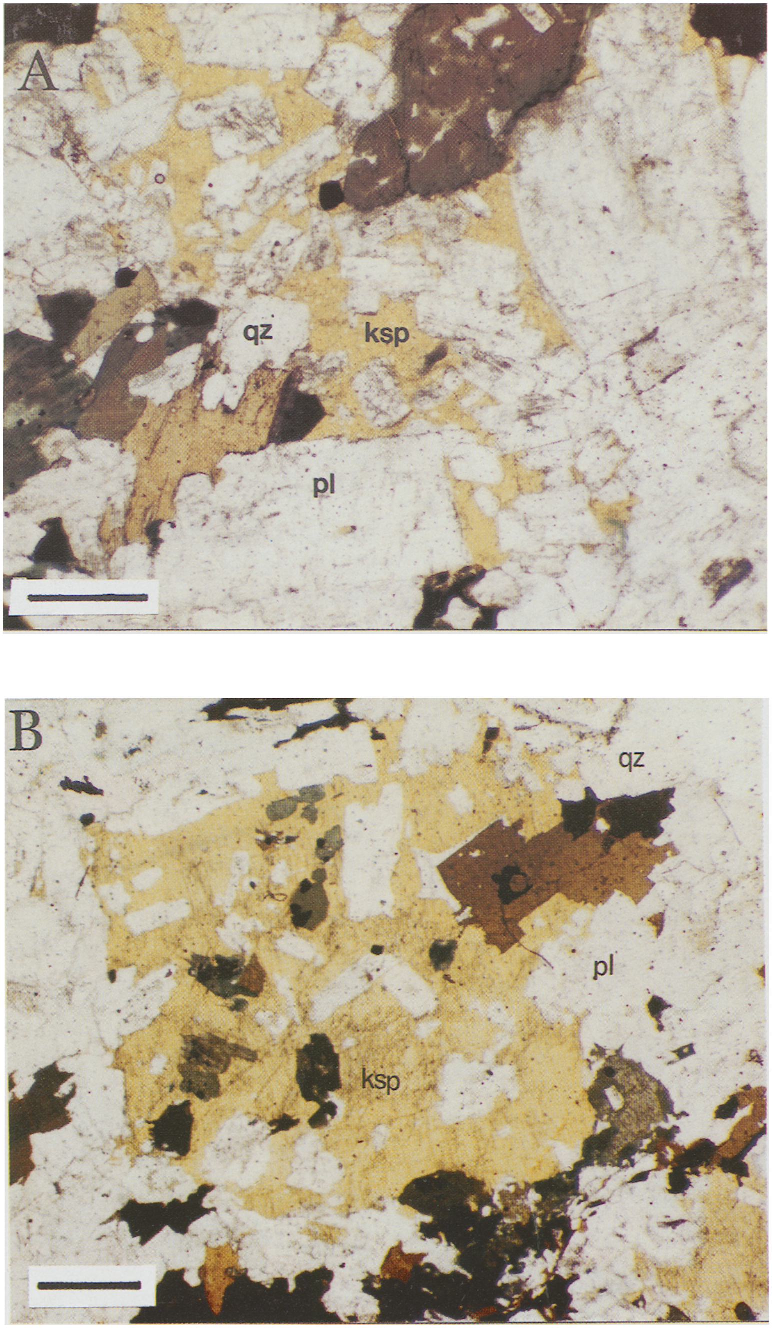

PLATE. 3. Plane-polarized light photomicrographs of the characteristic textures of the Arequipa and Yauca granodiorites from the Peruvian Coastal Batholith. The alkali feldspar in both sections has been stained yellow using sodium cobaltinitrite. Scale bar represents 1 mm in both photomicrographs. (A) Arequipa granodiorite: plagioclase crystals form a touching framework along with some quartz crystals. Alkali feldspar is restricted to the interstices. (B) Yauca granodiorite: alkali feldspar 'plate' containing numerous inclusions of the other major phases. The surrounding framework is dominated by plagioclase and some quartz crystals.

euhedral to subhedral tabular crystals which form a touching framework in two dimensions. Quartz forms both equant anhedral grains, and isolated interstitial pockets. It is the alkali feldspar morphology and geometry which shows significant differences between the two samples. In the Arequipa granodiorite, alkali feldspar crystals always occur as isolated interstitial pockets (Plate 3*a*), some of which show optical continuity. However, in the Yauca sample, alkali feldspar forms large 'plates' up to 10 mm in diameter that display highly anhedral margins and contain randomly oriented inclusions of all the other major phases (Plate 3*b*). Many of these inclusions are isolated from one another in two-dimensions.

The morphology and geometry of the plagioclase in both textures clearly implies that it was the earliest phase to crystallize and contributed substantially towards the growth of a crystal framework. Quartz appeared later than plagioclase, locally contributing to framework development but also crystallising interstitially. The nucleation and growth of alkali feldspar in the Arequipa granodiorite appears to have been restricted to the interstices of the crystalline framework. In the Yauca granodiorite, the large plate-like form of the alkali feldspar and the isolated appearance of many of the inclusions suggests nucleation and growth at an earlier stage of crystallization, i.e. before development of a crystal framework.

Textural relations in three-dimensions

Plagioclase is the main framework-forming phase in both the Arequipa and Yauca granodiorite, forming an interconnected skeleton that is continuous through the texture (Figs 2 and 3). However, in the Arequipa sample (Fig. 2), it is possible to make a clear distinction between the larger crystals which can often be traced through four or five consecutive sections (> 2 mm), and smaller crystals which only appear in single sections (< 500 μm). These smaller crystals typically are found to be inclusions within other phases, and are considered to have been isolated from the melt at an early stage in their growth history. The continued growth of the framework crystals to late stage is evident from the anhedral overgrowths on crystal margins. These contrast with the euhedral outline of internal growth zones, which show that the early growth of most of the plagioclase crystals was unrestricted. The problems of determining the contiguity of crystals based solely on a 2-D surface can be seen in the Yauca sample (Fig. 3). The cluster of four plagioclase crystals are connected through the stack, yet in only two of the five serial slices do the crystals appear to touch. If presented with sections 1, 2 or 3, it would not be possible to say if any, or all, of the crystals were touching, or how they related to one another in the third dimension.

Alkali feldspar growth in the Arequipa sample was restricted to the pore spaces within the plagioclase framework (the alkali feldspar geometries in Fig. 4 are complementary to those in Fig. 2). Despite their isolated appearance in two-dimensions, interstitial pockets can be traced through up to six consecutive sections (Fig. 4), forming a continuum through the framework in the third-dimension. This indicates that much of the growth of alkali feldspar occurred in pore- spaces that were inter-connected during the stages prior to porosity occlusion (cf. Stage 3.1 in Fig. 1). In several of the images, there are small pockets of the alkali feldspar that are isolated from the large poikilitic crystal but in optical continuity (e.g. Section 3 in Fig. 4). In many cases these pockets are absent in both the overlying and underlying sections. These are interpreted as 'branches' from the main crystal and may represent slightly later alkali feldspar growth into restricted or dead-end pores (Stage 3.2 in Fig. 1). Unfortunately we do not see either the 'pore-ends' of the branches, or their attachment to the main crystal (although this technique is useful for interpreting the contiguity of the various elements, it should be remembered that it still only generates 2-D surfaces through the 3-D texture, and interpolation between these surfaces is still very much the realm of the trained eye).

The alkali feldspar crystals in the Yauca granodiorite appear as large anhedral plates up to 10 mm in diameter in thin section. In three-dimensions, individual crystals can be traced through consecutive sections (Fig. 5). Unlike the Arequipa granodiorite, the crystals do not form a contiguous network in three-dimensions, but are isolated from one another and appear 'suspended' within the texture. The crystal shown in Fig. 5 is present in seven consecutive sections, implying a depth of ~ 3 mm. However, this value should be taken as a minimum because the front end of the crystal was not sectioned (section 2 is the largest and is probably close to the centre). The crystal shows a highly anhedral rim, which is present in all the sections, and is evidence for continued growth to late in the crystallization interval. The inclusions within the alkali feldspar crystals are always un-orientated and do not appear to connect through any of the sections, indicating that much of the growth of alkali feldspar occurred towards the end of the crystal suspension stage (Stage 1 in Fig. 1).

Crystallization history

Semi-quantitative information on the crystallization history of felsic minerals in crystallizing granitic

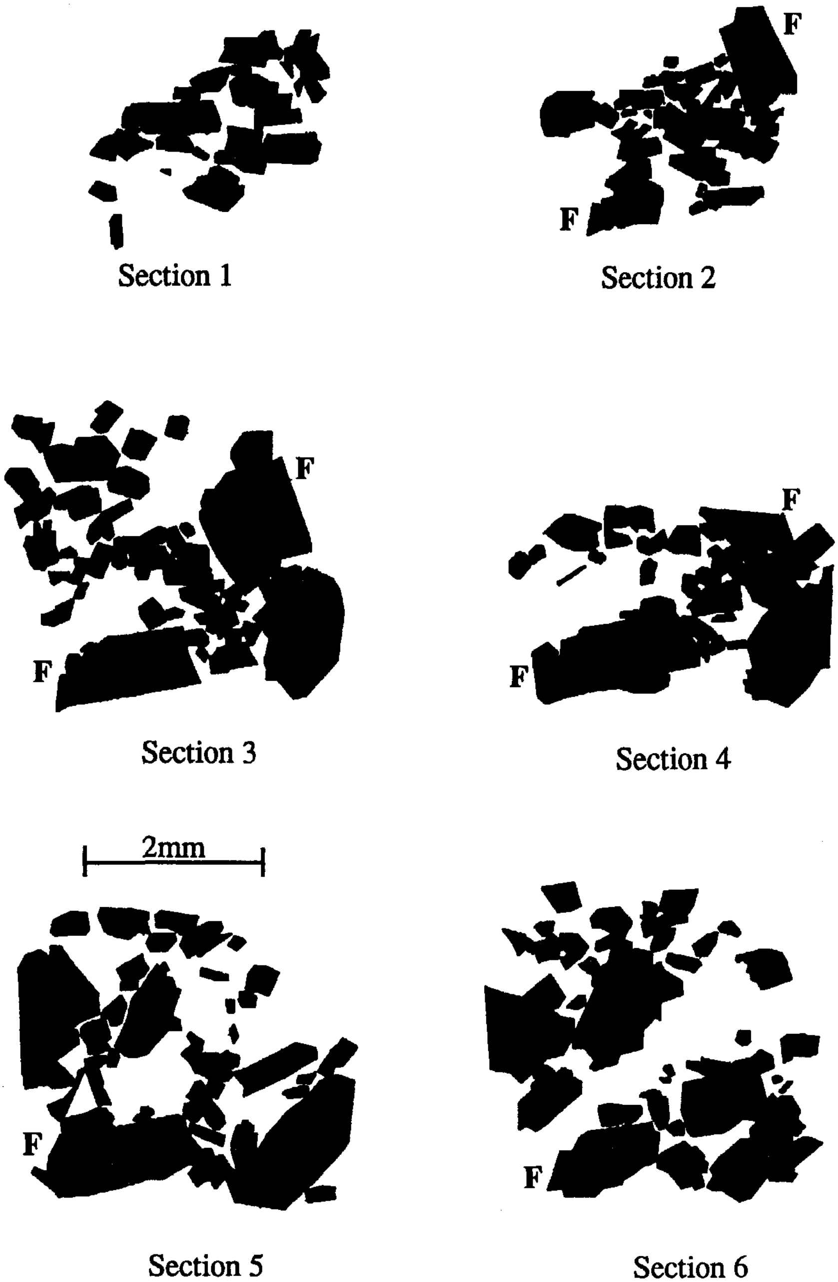

FIG. 2. Plagioclase geometries from six serial sections through the Arequipa granodiorite of the Peruvian Coastal Batholith. The distance between each of the sections is approximately 500 μm (total depth of 2.5 mm). Several of the larger 'Framework' crystals that are continuous through the sections have been labelled.

systems can be obtained from the quaternary An–Ab–Or–Qz system providing normative anorthite, albite, orthoclase and quartz contents are greater than 80% (Presnall and Bateman, 1973). As this is the case for both the samples described here, it is possible to compare the 3-D textural relations with

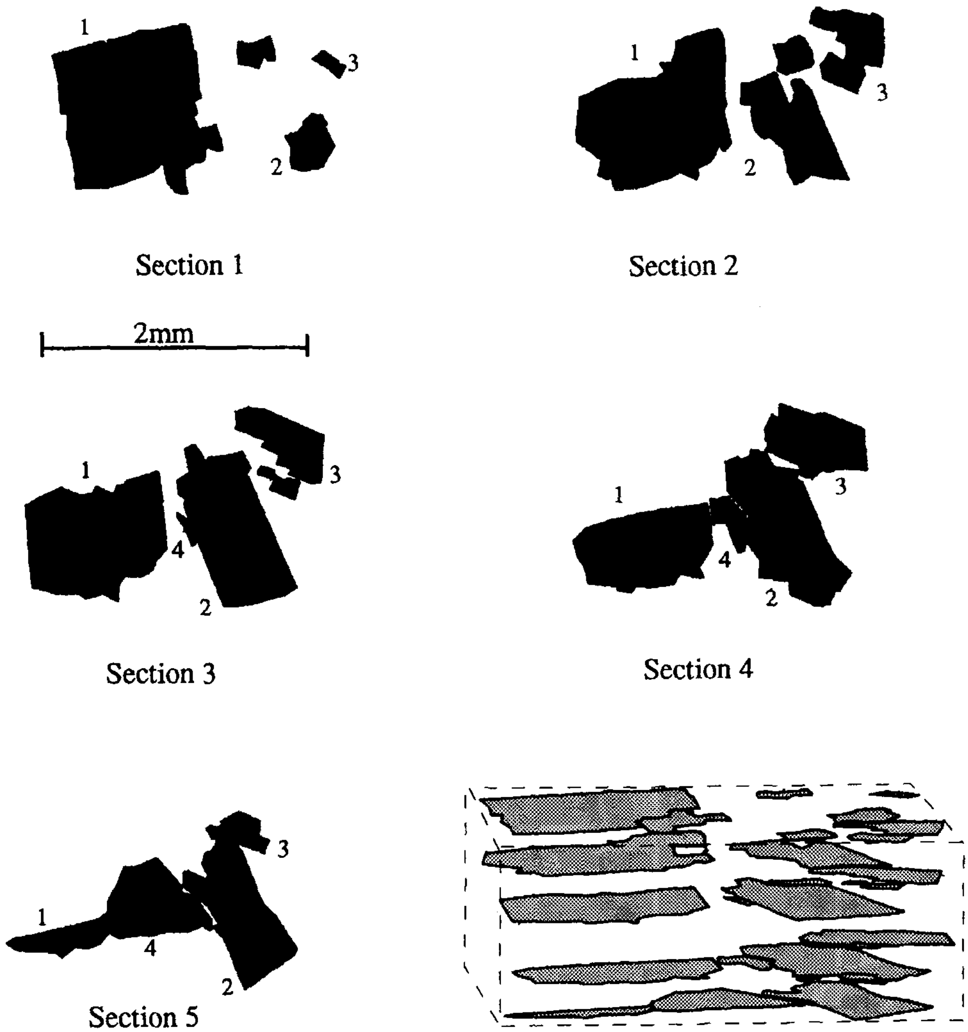

FIG. 3. Five consecutive sections through four plagioclase crystals from the Peruvian Coastal Batholith. The crystals form a touching framework *in three-dimensions*, although this is only evident in the last two sections (4 and 5). The distance between each of the sections is approximately 500 μm.

the predicted crystallization pathways of the felsic phases within the quaternary system (Fig. 6).

The CIPW normative compositions of both samples lie within the trivariant plagioclase volume (Fig. 6*a*). This is consistent with the early growth of plagioclase and its major contribution to framework development. Crystallization of quartz and alkali feldspar will have started as the melt evolved to the plagioclase/quartz divariant surface and the cotectic respectively. The order of crystallization in both rocks was, therefore, plagioclase, plagioclase + quartz, plagioclase + quartz + alkali feldspar.

The pathways of both melts through the system can be used to estimate the timing of first appearance of quartz and alkali feldspar through the crystallization interval relative to plagioclase. Both samples lie at approximately the same distance from the plagioclase/quartz divariant surface in the plagioclase

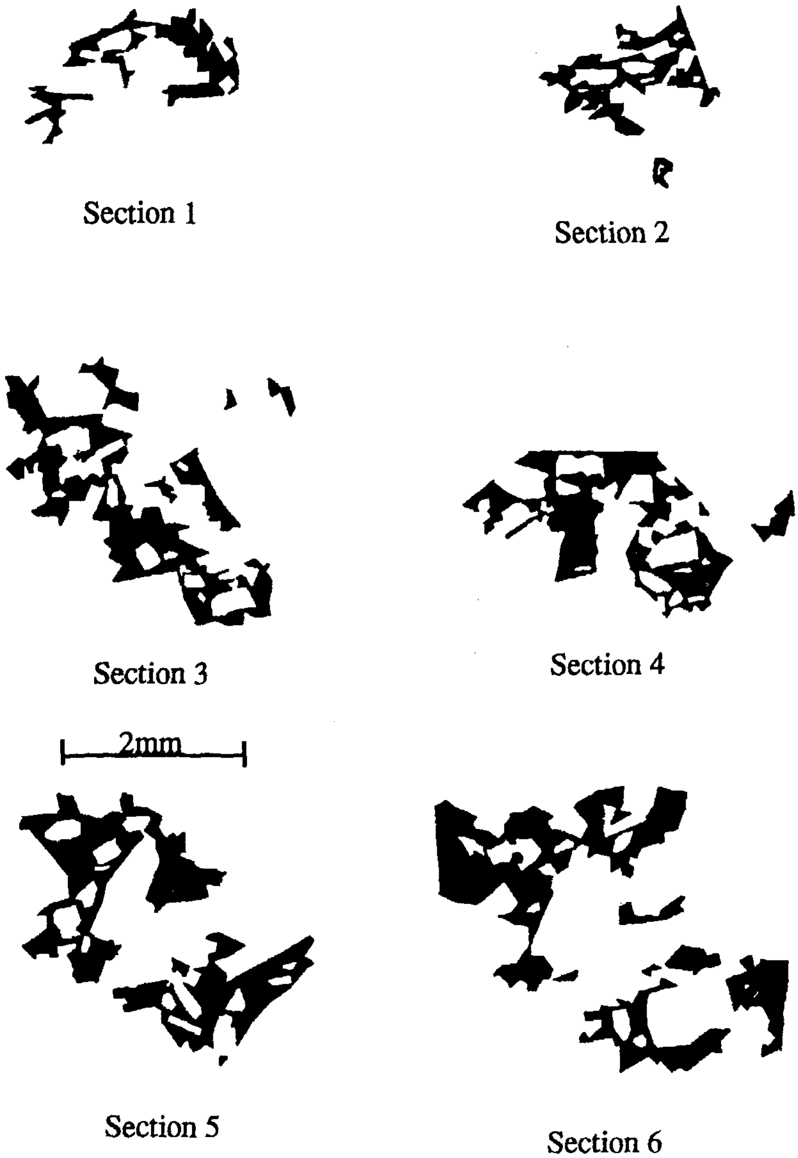

FIG. 4. Interstitial alkali feldspar geometries from six consecutive sections through the Arequipa granodiorite (the sections are complementary to those in Fig. 2). The alkali feldspar is in optical continuity through all of the sections and is therefore interpreted as one single poikilitic crystal that nucleated and grew before the pore spaces became isolated (Stage 3.3 in Fig. 1).

volume (Fig. 6*a*). However, the bulk composition of the Arequipa sample lies higher in the plagioclase volume (and hence further from the cotectic) than the Yauca sample, and will therefore have evolved to cotectic saturation later in the crystallization interval, i.e. alkali feldspar appeared at a lower melt-fraction in the Arequipa granodiorite. This is consistent with the 3-D textural evidence for the appearance of alkali feldspar before, and after framework development in the Yauca and Arequipa granodiorites respectively (Fig. 6*b*).

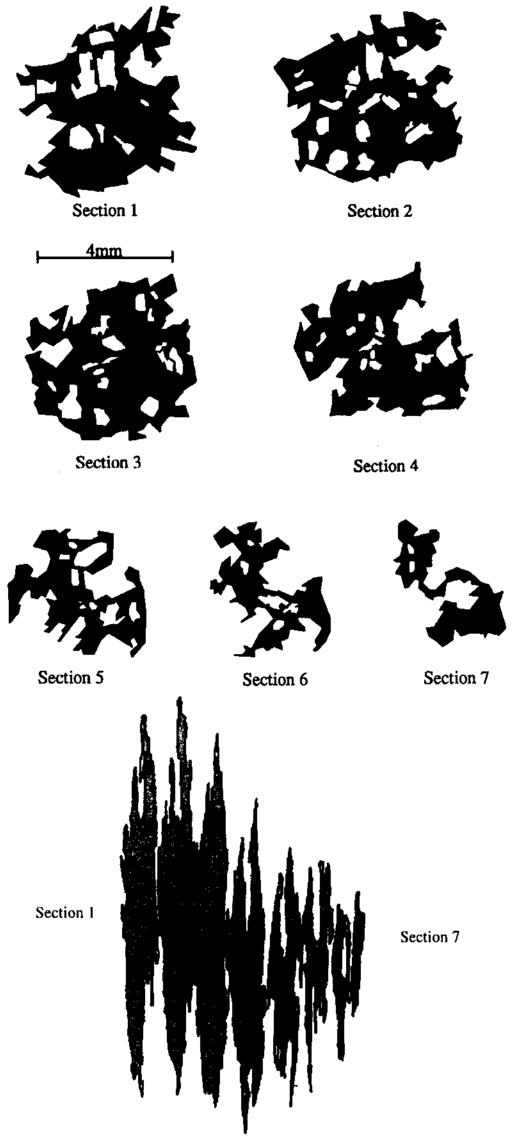

FIG. 5. The geometry of a single alkali feldspar crystal through seven serial sections through the Yauca granodiorite. The location of the included crystals has also be shown. Despite the anhedral geometry at the margin, the crystal shows a high sphericity and has a minimum depth of 3 mm (approximate distance between each section is 500 μm). The isolated appearance of the inclusions, and the overall equant geometry of the crystal, is evidence for the onset of growth before framework development.

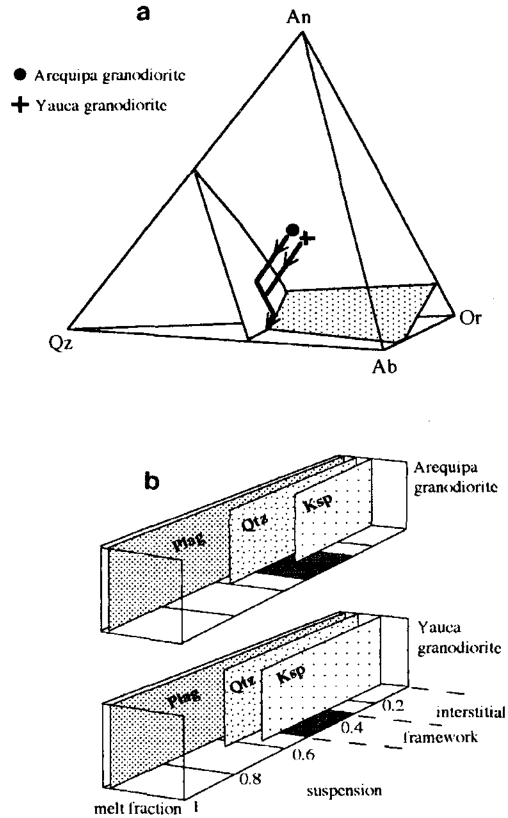

FIG. 6. The bulk compositions and predicted crystallization pathways of the Arequipa and Yauca granodiorites in the quaternary An–Ab–Or–Qz system (6*a*). It should be noted that the system only accounts for the felsic phases and therefore cannot be used to accurately determine melt pathways, which are often partially controlled by mafic phases (e.g. hornblende and biotite) (Heltz, 1976). Both samples lie in the plagioclase volume and will have evolved to three-phase saturation via the plagioclase/quartz divariant surface. The predicted crystallization sequence of plagioclase; plagioclase + quartz; plagioclase + quartz + alkali feldspar, is consistent with the history deduced from the textural relations in three-dimensions (6*b*).

Summary

The 3-D observations presented here have provided insights into the development of the textures of granitic rocks, in particular the development of crystal frameworks, the timing of nucleation and growth of phases from pores within the framework, and the restriction, isolation and occlusion of the melt-filled porosity. We have shown that the crystallization histories of the felsic phases in two Peruvian granodiorites, as deduced from the three-dimensional study of the textures (Fig. 6*b*), are consistent with the predicted evolution of their parent melt based on known phase relationships (Fig 6*a*). This is an important conclusion, since it provides a basis for studying the generation and evolution of compositional zonation in siliceous magma chambers, specifically, the movement of melt away from the crystal framework through interconnected pore spaces. Furthermore, the static model of crystallization allows inferences to be drawn regarding the rheology of the granite during its crystallization interval, and provides the basis for understanding other granitic systems that have deformed during emplacement and crystallization. This work has shown how serial thin sectioning, image analysis and three-dimensional reconstruction techniques can be used in such studies, and has highlighted some of the problems of interpolating two-dimensional information from thin section into the third dimension.

Acknowledgements

The design of the hardware and development of the software used in parts of this study were undertaken in conjunction with D.P. McKenzie and M. Spiegelman at Cambridge. This work has been supported at Cambridge and Liverpool by the NERC. Special thanks go to Nick Petford and Mike Cheadle for their support and comments, and to Richard D'Lemos and Ed Stephens for significantly improving the original manuscript.

References

Atherton, M. P. (1981) Horizontal and vertical zoning in the Peruvian Coastal Batholith. *J. Geol. Soc. Lond.*, **138**, 343–9.

Atherton, M. P. and Brenchley, P. J. (1972) A preliminary study of the structure, stratigraphy and metamorphism of some contact rocks of the Western Andes, near Quebrada Venado Muerto, Peru. *Geol. J.*, **8**, 161–78.

Atherton, M. P. and Sanderson, L. M. (1985) The chemical variation and evolution of the superunits of the segmented Coastal Batholith. In *Magmatism at a plate edge: the Peruvian Andes* (Pitcher, W.S., Atherton, M.P., Cobbing, E.J. and Beckinsale, R.D., eds). Blackie, Halstead Press, Glasgow, pp. 108–18.

Atherton, M. P., McCourt, W. J., Sanderson, L. M. and Taylor, W. P. (1979) The geochemical character of the segmented Peruvian Coastal Batholith and associated volcanics. In *Origin of Granite Batholiths: geochemical evidence* (Atherton, M.P. and Tarney, J., eds). Shiva Publ. Co., Orpington, Kent, pp 45–64.

Bryon, D. N. (1992) *Textural development in granitoid rocks: a case study from the zoned Linga superunit of the Coastal Batholith, Peru.* PhD thesis, Univ. of Liverpool (unpubl).

Bryon, D. N., Atherton, M. P. and Hunter, R. H. (1994) The description of the primary textures of Cordilleran granitic rocks. *Contrib. Mineral. Petrol.*, **117**, 66–75.

Cooper, M. R. and Hunter, R. H. (1995) Precision serial lapping, imaging and three-dimensional reconstruction of minus-cement and post-cementation intergranular pore-systems. *Mineral. Mag.*, **59**, 213–220.

Heltz, R. T. (1976) Phase relations of basalts in their melting range at P_{H_2O} = 5 kb, Part II. Melt compositions. *J. Petrol.*, **17**, 139–93.

Hunter, R. H. (1987). Textural equilibrium in layered igneous rocks. In *Origins of igneous layering* (Parsons, I., ed). D. Reidel Publ. Co., Dordrecht, pp 473–503.

Means, W. D. and Park, Y. (1994) New experimental approach to understanding igneous texture. *Geology*, **22**, 323–6.

Presnall, D. G. and Bateman, P. C. (1973) Fluid inclusion relations in the system $NaAlSi_3O_8$–$CaAl_2Si_2O_8$–SiO_2–H_2O and generation of granite magmas in the Sierra Nevada Batholith. *Geol. Soc. Amer. Bull.*, **84**, 3181–202.

Streckeisen, A. L. (1976) To each plutonic rock its proper name. *Earth Sci. Rev.*, **12**, 1–33.

Wager, L. R., Brown, G. M. and Wadsworth, W. J. (1960) Types of igneous cumulates. *J. Petrol.*, **1**, 73–85.

[*Revised manuscript received 24 August 1994*]